10-16-2013

A New Solid Oxide Molybdenum–Air Redox Battery

Xuan Zhao

Yunhui Gong

Xue Li

Nansheng Xu

Kevin Huang
University of South Carolina - Columbia, huang46@cec.sc.edu

Publication Info

Published in *Journal of Chemistry A*, Volume 1, Issue 48, 2013, pages 14858-14861.

Journal of Materials Chemistry A

RSC Publishing

COMMUNICATION

View Article Online
View Journal | View Issue

A new solid oxide molybdenum–air redox battery†

Xuan Zhao, Yunhui Gong, Xue Li, Nansheng Xu and Kevin Huang*

Cite this: *J. Mater. Chem. A*, 2013, **1**, 14858

Received 14th July 2013
Accepted 15th October 2013

DOI: 10.1039/c3ta12726e

www.rsc.org/MaterialsA

A new type of rechargeable molybdenum–air battery based on the technologies of reversible solid oxide fuel cells and chemical looping is reported in this study. The reversible solid oxide fuel cell serves as the electrical unit to realize the charging and discharging cycles while a pair of Mo/MoO_2 redox couple integrated with the reversible solid oxide fuel cell stores electrical energy *via* an H_2–H_2O oxygen shuttle. The specific charge of the new battery reaches 1117 A h per kg-Mo at 550 °C, which is 45% higher than the non-rechargeable Mo–air battery. The corresponding discharge specific energy is 974 W h per kg-Mo with a round trip efficiency of 61.7%. In addition, the new Mo–air redox battery also exhibits 13.9% and 24.5% higher charge density (A h L^{-1}) and energy density (W h L^{-1}) than the state-of-the-art solid oxide Fe–air redox battery, respectively.

High capacity rechargeable batteries are highly desirable for cost-effective and energy-efficient electrochemical energy storage systems. Batteries with metal–air chemistry have a great potential to meet this demand due to their intrinsically high specific energy and needless storage for the air–electrode reactant.[1–5] Throughout the literature, it is interesting to note that almost all the existing metal–air batteries exclusively use ionic solutions as the electrolytes, two examples of which are alkaline (OH^-) for Zn–air and Li-salts (Li^+) for Li–air. While the high ionic conductivity and fast electrode kinetics at the liquid/solid-electrode interfaces can facilitate the metal–air batteries to achieve high energy capacity, a number of chemical problems remain to be solved before they can become commercially viable. First, the interactions between the electrolyte solutions and solid electrodes readily occur, causing capacity fade. Second, the charge carriers such as OH^- and Li^+ can lead to the formation of condensed phases (*e.g.* $Zn(OH)_2$ and Li_2O or Li_2O_2) on the surfaces of either negative or positive electrode (air-electrode), blocking reactive sites for a sustained electrochemical reaction. The higher the rate of cycling, the faster the above processes would be. The significant kinetic irreversibility has considerably undermined the prominent thermodynamic advantage inherited by the metal–air batteries.

To cope with these problems, we have recently argued that the use of a solid oxide-ion conductor, *e.g.*, Y_2O_3-doped ZrO_2 (YSZ) and Sr- and Mg-doped $LaGaO_3$ (LSGM), as the electrolyte in a solid oxide fuel cell (SOFC) can effectively circumvent the aforementioned problems facing the conventional metal–air batteries.[6–13] First, oxide-ion conductors are usually very stable when in contact with a variety of different oxides under operation and fabrication conditions. Second, only gaseous O_2 is involved in the air-electrode reaction, thus avoiding blockage of air-pathways established by a prefabricated porous electrode structure. We subsequently tested the concept in a battery configuration using a traditional reversible solid oxide fuel cell (RSOFC) as the "electrical functional unit (EFU)" in conjunction with a pair of metal/metal-oxide redox couples as the energy storage medium (ESM) with encouraging results.[6–13] To facilitate the redox reactions, a mixture of H_2 and H_2O is also utilized as the oxygen shuttle gas to promote the redox reaction. The battery of this kind is generally termed solid oxide metal–air redox battery (SOMARB).

In addition to the avoidance of stability issues of the conventional metal–air batteries, the SOMARB also has a distinctive advantage in that the electrode no longer serves as a medium of energy storage. Instead, the chemical energy is stored inside the metal/metal-oxide redox couple that is physically separated from but next to the fuel-electrode. This design not only entitles the battery to perform high-rate cycles without invoking damages to cell structures from volume changes, but also allows for new metal–air chemistry to be conveniently explored through a simple exchange of redox couple materials. Therefore, in addition to the first-generation Fe–air redox batteries based on Fe–FeO_x redox couples,[6–8,10–13] we have recently investigated a high energy density W–air redox battery

Department of Mechanical Engineering, University of South Carolina, Columbia, SC29201, USA. E-mail: kevin.huang@sc.edu; Fax: +1 803 777 0106; Tel: +1 803 777 4185

† Electronic supplementary information (ESI) available: Experimental details. See DOI: 10.1039/c3ta12726e

using the W–WO_2 redox couple as the ESM.[9] A similar work was also reported on a Mg–air battery, although it was non-rechargeable due to a poor kinetic reversibility of the Mg–MgO redox couple.[14] While new SOMARBs are being reported, those with higher capacity and better reversibility operated at reduced temperatures remain to be demonstrated.

Here, we report for the first time on a high capacity and reversible solid oxide Mo–air redox battery operated at low temperatures; the battery uses a Mo–MoO_2 redox couple as the ESM and an RSOFC as the EFU. Its configuration and working principle with H_2–H_2O as the oxygen shuttle gas are illustrated in Fig. 1. The phase diagram of the Mo–O system illustrating the chemical stability of the Mo–MoO_2 redox couple can be found in Fig. S1 (ESI).†

The ability to be recharged for the new Mo–air redox battery is clearly an advantage over a recently reported non-rechargeable Mo–air battery;[15,16] the latter uses Mo as the negative electrode and an alkali (KOH) as the electrolyte, producing a specific charge (A h kg^{-1}) 2.5 times (~770 A h per kg-Mo) higher than the commercial Zn–air batteries.[15,16] However, as aforementioned, the use of liquid-based electrolytes in this battery can invoke deleterious reactions with electrode materials and formation of electrochemically blocking condensed phases on the surface of the electrode, resulting in performance instability.

The Mo–O_2 chemistry has both thermodynamic and kinetic advantages over other metal–O_2 counterparts for SOMARBs. Due to the heavy nature of Mo (ρ = 10.28 g cm^{-3}) and a large oxygen/metal ratio in MoO_2, the maximum theoretical specific energy (MTSE) (W h kg^{-1}) and maximum theoretical energy density (MTED) (W h L^{-1}) derived from the Mo–O_2 chemistry are intrinsically higher.[9] Fig. 2 compares the thermodynamic properties calculated for Mo–MoO_2, Fe–Fe_3O_4 and W–WO_2 redox couples. It is evident that the Mo–MoO_2 redox couple displays the highest MTED (Fig. 2(a)) and almost twice the MTSE over the W–WO_2 redox couple (Fig. 2(b)). Despite exhibiting slightly lower MTSE than Fe–Fe_3O_4 (Fig. 2(b)), Mo–MoO_2 possesses a higher EMF than Fe–Fe_3O_4 (Fig. 2(c)). These thermodynamic results suggest that Mo–MoO_2 could be a potential redox couple for high performance solid oxide Mo–air redox batteries.

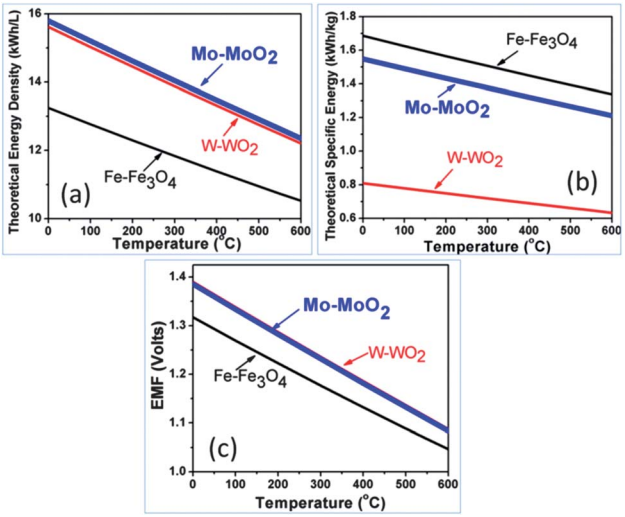

Fig. 2 Comparison of thermodynamic properties of (a) maximum theoretical energy density (kW h L^{-1}), (b) maximum theoretical specific energy (kW h kg^{-1}), and (c) EMF among Fe–Fe_3O_4, W–WO_2 and Mo–MoO_2 redox couples calculated as a function of temperatures.

The kinetic advantage of Mo–O_2 chemistry is manifested by the high kinetic rate constants of the Mo–MoO_2 redox reaction. Fig. 3 shows the maximum charge density (Q_{max}, A h L^{-1}), maximum specific charge (q_{max}, A h g^{-1}) calculated for the Mo–MoO_2 redox couple, and maximum current density (J_{max}, A cm^{-2}) operated by RSOFC in match with the kinetic rate constants of the Mo–MoO_2 redox reaction. In the ESI,† we provide details on how these kinetic parameters are calculated. These parameters represent the upper limits to the charge and energy capacities achievable by the battery. For comparison, the

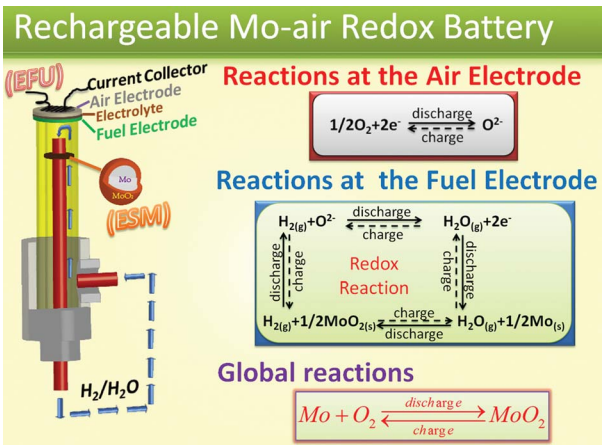

Fig. 1 Schematic of the configuration and working principle of the solid oxide Mo–air redox battery.

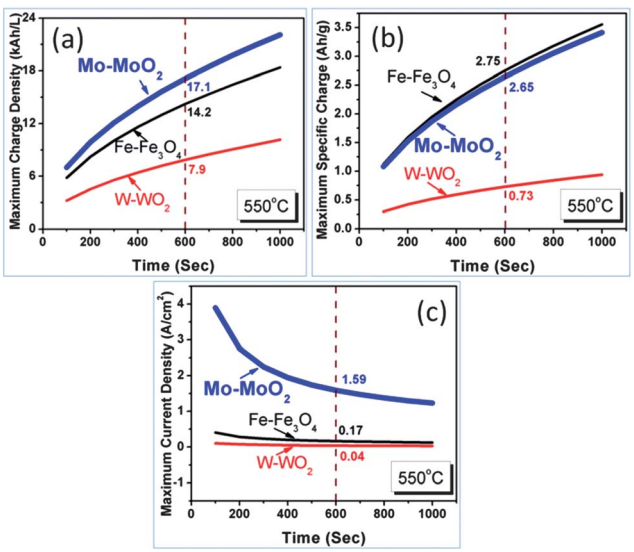

Fig. 3 Maximum charge density Q_{max}(a), maximum specific charge q_{max} (b), and maximum current density J_{max} of RSOFC sustained by Mo–MoO_2, Fe–Fe_3O_4 and W–WO_2 operated at 550 °C.

same properties are also calculated for Fe–Fe_3O_4, and W–WO_2 redox couples, and shown in Fig. 3. It is evident that Mo–MoO_2 possesses the best kinetic attributes in terms of being an efficient redox couple for chemical storage, despite slightly lower maximum specific charge than the Fe–Fe_3O_4 redox couple.

The energy storage characteristics of the new solid oxide Mo–air redox battery operated at 550 °C are shown in Fig. 4. To ensure the best RSOFC performance at this temperature, we employed the Sr- and Mg-doped $LaGaO_3$ (LSGM) as a solid electrolyte; it has higher oxide-ion conductivity than Y_2O_3-stabilized ZrO_2 (YSZ), particularly in the IT range.[10,17–20] To demonstrate proof-of-concept, the battery was cycled at J = 10 mA cm^{-2} for 10 consecutive cycles. For each single discharge or charge cycle, the duration was set as 10 min. It should be noted that the specific energy shown in Fig. 4 was normalized to the mass of the actually consumed Mo by the oxygen flux (corresponding to the current) for the redox reactions. Such normalization allows for comparison with theoretical values such as those shown in Fig. 2 and other published results. According to Fig. 4(a), the battery produces an average specific charge of 1117 A h per kg-Mo, which is 45% higher than the primary Mo–air batteries.[15,16] Fig. 4(b) further shows that the battery has an average discharge specific energy of 974 W h per kg-Mo, which is roughly 78.5% of the MTSE. The measured EMF is 1.108 V, which agrees with the theoretical value (=1.108 V). The average round trip efficiency is 61.7% over ten consecutive cycles when compared to the charge specific energy (=1578 W h per kg-Mo). The lower round-trip efficiency and specific energy in relative to the MTSE suggest the occurrence of the energy loss to the polarization of RSOFC and kinetic resistance of the Mo–MoO_2 redox reactions. These energy losses can be minimized by optimizing the performance of RSOFC and increasing the surface area of ESM. Overall, no significant degradation is observed during the 10-cycles period.

The higher charge/energy density (A h L^{-1}, W h L^{-1}) of the Mo–air redox battery than the previously reported model Fe–air counterpart is further illustrated in Fig. 5. The average charge density of the Mo–air redox battery is 11.5 kA h per L-Mo, which is 13.9% higher than that of the Fe–air redox battery (=10.1 kA h per L-Fe). Similarly, the average energy density of the Mo–air redox battery shows 24.5% higher than the Fe–air redox battery. Not shown in Fig. 5 are the average round-trip efficiency and EMF of the Fe–air battery, which are 60.9% and 1.067 V, respectively. The higher energy density, round-trip efficiency and EMF of the Mo–air battery are consistent with the thermodynamic and kinetic predictions presented in Fig. 2 and 3.

In summary, the present study demonstrates that the new solid oxide Mo–air redox battery has a great potential to be a high capacity and reversible battery system for mid-to-large-scale stationary energy storage. Its new metal–air chemistry based on solid oxide-ion electrolytes overcomes the critical problems facing conventional liquid-electrolyte based metal–air batteries. The unique design of separated EFU and ESM allows the new battery to perform electrical cycles at high rates without invoking damages to the cell structure from the volume changes. The elegant balance between thermodynamics and kinetics in the Mo–MoO_2 ESM has led to the demonstration of a specific charge as high as 1117 A h per kg-Mo at 550 °C, 45% higher than the non-rechargeable Mo–air battery. The corresponding discharge specific energy reaches 974 W h per kg-Mo, 78.5% of the MTSE, at a round trip efficiency of 61.7%. When compared to the standard solid oxide Fe–air redox battery, the Mo–air redox battery exhibits 13.9% and 24.5% higher charge density and discharge energy density, respectively. The round-trip efficiency of the Mo–air redox battery is also better than the Fe–air redox battery. However, it is recognized that the gap between the observed performances and the theoretical predictions caused by energy losses to the polarizations of RSOFC and kinetic resistances of redox reactions in ESM needs

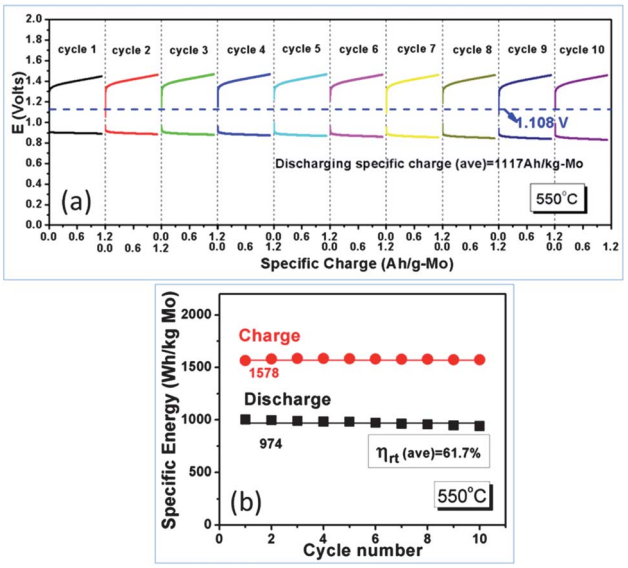

Fig. 4 Electrochemical performance of the solid oxide Mo–air redox battery operated at 550 °C for 10 consecutive cycles under a current density of 10 mA cm^{-2}. (a) Voltage *vs.* capacity and (b) average specific energy *vs.* number of cycles.

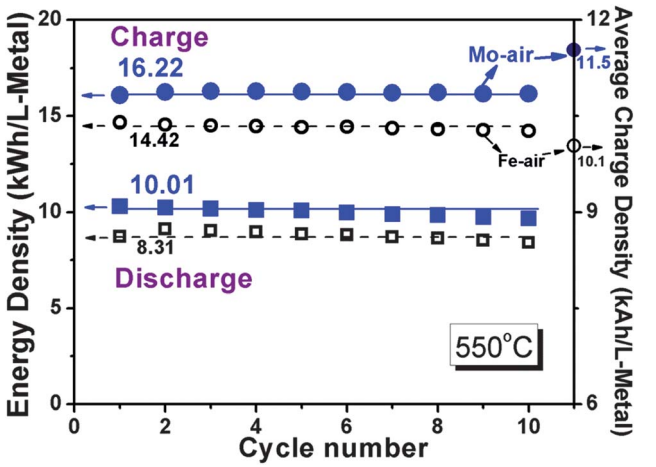

Fig. 5 Comparison of energy density and charge density as a function of number of cycles for the Mo–air and Fe–air redox batteries. Blue: Mo–air and black: Fe–air.

to be narrowed. An on-going research in our lab is aimed to minimize these losses and further extend the number of stable cycles to the level of commercial applicability.

Experimental section

Preparation of redox couple materials

The functional redox precursor MoO_3 in the Mo-based ESM was chosen from a commercial molybdenum trioxide (MP Biomedicals, LLC). The MoO_3 was first ball-milled into fine particles, followed by mixing with V-006A (Heraeus) to form a paste. The paste was then screen-printed onto a Ni-foil support and calcined in open air at 650 °C for 2 h. The Fe-based ESM was synthesized from a co-precipitation method.[6–8] Thus obtained Fe_2O_3–ZrO_2 (Fe : Zr = 85 : 15, atomic ratio) powders were then ball-milled to break up the soft agglomeration, followed by mixing with V-006A (Heraeus) to form the Fe-based paste. The paste was then screen-printed onto a Ni-foil support and calcined in open air at 650 °C for 2 h. CeO_2 nanoparticles were finally dispersed into the aforementioned Fe-based ESM as previously described.[10]

Battery assembly

A simple planar button cell configuration was used for the battery testing, the configuration which is similar to that described in ref. 7. An LSGM electrolyte-supported button cell with an effective electrode area of 1.3 cm^2 was used as the RSOFC.[15] The structure of the RSOFC is illustrated in Fig. S2.† The compositions and dimensions of the components in this RSOFC are summarized in Table S1.† Pt and silver meshes were used as current collectors for the fuel-electrode and air-electrode, respectively. A home-made glass-ceramic was used as the sealant.

Testing procedure

During heating, the starting material MoO_3 was first reduced with a mixture gas of 5%H_2–N_2 + 3%H_2O. As the glass sealant melted around 650 °C, the protective gas was switched to H_2–3%H_2O to fully reduce MoO_3 into metallic Mo. After approximately half an hour of holding at 650 °C to allow the glass sealant to settle, the temperature was then gradually ramped down to the testing temperature of 550 °C. During the ramping down, impedance spectra and *V–I* curves were recorded as a fuel cell. When the system was finally stabilized at 550 °C, the fuel-electrode chamber was then closed, followed by applying a small discharge current to pump oxygen from air to fuel-electrode to oxidize Mo to MoO_2 and to establish the Mo–MoO_2 equilibrium. The overall process was constantly monitored by observing the cell's OCV. The equilibrium OCV is roughly 1.108 V at 550 °C. As soon as the cell OCV reached this value, the electrical cycles were started. After the test, the system was cooled down in an open system with a flowing 5%H_2–N_2 + 3% H_2O gas mixture. Readers can refer to our previous publication for more details.[10]

Notes and references

1 Z. Peng, S. A. Freunberger, Y. Chen and P. G. Bruce, *Science*, 2012, **337**, 563.
2 O. Chusid, Y. Gofer, H. Gizbar, Y. Vestfrid, E. Levi, D. Aurbach and I. Riech, *Adv. Mater.*, 2003, **15**, 627.
3 Y. C. Lu, H. A. Gasteiger and Y. Shao-Horn, *J. Am. Chem. Soc.*, 2011, **133**, 19048.
4 J. S. Lee, S. Tai Kim, R. Cao, N. S. Choi, M. Liu, K. T. Lee and J. Cho, *Adv. Energy Mater.*, 2011, **1**, 34.
5 S. R. Narayanan, G. K. S. Prakash, A. Manohar, B. Yang, S. Malkhandi and A. Kindler, *Solid State Ionics*, 2012, **216**, 105.
6 N. Xu, X. Li, X. Zhao, J. B. Goodenough and K. Huang, *Energy Environ. Sci.*, 2011, **4**, 4942.
7 X. Zhao, N. Xu, X. Li, Y. Gong and K. Huang, *RSC Adv.*, 2012, **2**, 10163.
8 X. Zhao, N. Xu, X. Li, Y. Gong and K. Huang, *ECS Trans.*, 2013, **45**, 113.
9 X. Zhao, X. Li, Y. Gong, N. Xu, K. Romito and K. Huang, *Chem. Commun.*, 2013, **49**, 5357.
10 X. Zhao, Y. Gong, X. Li, N. Xu and K. Huang, *J. Electrochem. Soc.*, 2013, **160**, A1241.
11 X. Zhao, N. Xu, X. Li, Y. Gong and K. Huang, *ECS Trans.*, 2013, **50**, 115.
12 X. Zhao, Y. Gong, X. Li, N. Xu and K. Huang, *J. Electrochem. Soc.*, 2013, **160**, A1716–A1719.
13 M. Guo, X. Zhao, R. E. White and K. Huang, *J. Electrochem. Soc.*, 2013, **160**, A2085–A2092.
14 A. Inoishi, Y. W. Ju, S. Ida and T. Ishihara, *Chem. Commun.*, 2013, **49**, 4691.
15 D. Chu, R. Jiang, J. Walker and J. C. W. Walker, US Patent 20100255375 A1, 2010.
16 D. Chu, R. Jiang and J. C. W. Walker, US Patent 8148020 B2, 2012.
17 X. Zhao, X. Li, N. Xu and K. Huang, *Solid State Ionics*, 2012, **214**, 56.
18 A. Inoishi, S. Ida, S. Uratani, T. Okano and T. Ishihara, *RSC Adv.*, 2013, **3**, 3024.
19 A. Inoishi, Y. Okamoto, Y. Ju, S. Ida and T. Ishihara, *RSC Adv.*, 2013, **3**, 8820.
20 A. Inoishi, S. Ida, S. Uratani, T. Okano and T. Ishihara, *Phys. Chem. Chem. Phys.*, 2012, **14**, 12818.